Bull. Disas. Prev. Res. Inst., Kyoto Univ., Vol. 37, Part 4, No. 328, December, 1987 147

Laboratory Tests of the Single- and Multiple-scattering Models for the Generation of Seismic Coda Waves

By Koji MATSUNAMI

(Manuscript received September 22, 1987)

Abstract

To investigate the scattering property of the earth's crust using seismic coda waves, scattering models for coda generation were first tested using an ultrasonic technique and sufficiently large 2-D models of scattering media. Next, short-period coda waves from local small earthquakes that occurred in the central Kinki district of southwest Japan were analyzed with the multiple-scattering model for coda generation given by Gao *et al.* The principal results obtained are (1) that the experiments demonstrate that the multiple-scattering model of Gao *et al.* for coda generation explains the time decay of the amplitude of coda consisting of waves scattered by small-scale crack-like heterogeneities in the earth's crust very well; (2) that when the lithosphere is assumed to be a scattering medium with randomly distributed heterogeneities, the isotropic scattering coefficient, g, of the earth's crust in the central Kinki district is nearly proportional to $f^{1.0}$ in the frequency range of $2<f<16$ Hz; and (3) that from the weak dependence of g on the frequency, such as $g \propto f^{0.7-1.2}$, for the earth's crust in seismically active regions, it is suggested that the heterogeneities responsible for short-period coda generation may be numerous cracks in the crust that have lengths of less than about 100 m.

1. Introduction

Extensive studies[1-7] have shown that most of the characteristics of the coda waves for local earthquakes can be explained by the single scattering of S waves. On the basis of the single-scattering theory[1,2], Aki[8] concluded that coda waves consist of S-to-S back-scattered waves from many randomly distributed heterogeneities in the lithosphere. Recently it has been reported that the single back-scattering model for coda generation does not explain the amplitude of coda waves[9,10]. Furthermore, Frankel and Clayton[11], using the finite-difference method, numerically showed that the single-scattering model of coda generation is not valid when scattering attenuation is moderate or large. Also, Menke and Chen[12] showed numerically that the fall off rate of net forward-scattered coda, including multiple-scattering interactions, is very different from that of single back-scattered coda. This observational and theoretical evidence shows that multiple scattered waves have an important function in seismic coda. Therefore, if we wish to use coda waves for more accurate estimations of the heterogeneities in the lithosphere, we must convert the single-scattering theory for the analysis of coda waves to a multiple-scattering one. In this study, therefore, to investigate the scattering property of the earth's crust, I attempted to analyze short-period seismic coda waves using the multiple-scattering model for coda generation.

Kopnichev[13] and Gao *et al.*[14] independently formulated the time decay of coda

energy density at a hypocenter, respectively taking into account the effect of scattering up to 3rd and 7th orders, and using their formulas, investigated the contribution of multiple scattering to the coda. It is important to ascertain that the single-scattering model used widely so far, as well as the multiple-scattering models are applicable to what strength of scattering in media, before using the multiple-scattering models for coda analysis. To test the scattering models for coda generation, it is very difficult to correctly synthesize seismograms theoretically that have a long coda showing multiple-scattering effects. One alternative to the theoretical method is to produce seismograms in laboratory experiments for sufficiently large two-dimensional models of scattering media from ultrasonic data. Seismograms made in this manner include all the multiple-scattered waves and have long codas. Therefore, if we can devise a good analog model of the lithosphere that shows various kinds of heterogeneities, the method could be used to test scattering models for coda generation. Thus, in this study, I first tested scattering models for coda generation by laboratory experiments before analyzing seismic coda waves.

When we make lithosphere models as scattering media, we must know what kind of heterogeneities is responsible for coda generation. So far, however, because of insufficient knowledge about the heterogeneities that exist in the lithosphere, many researchers have assumed that the lithosphere is a random medium and have attempted to deduce the parameters of the heterogeneities statistically. Wu and Aki[15] formulated elastic wave scattering through a random medium, using the Born approximation. After comparing the theoretical values with their observations, they concluded that the short-period coda waves of local earthquakes are generated by back scattering or by large-angle-scattering of small-scale (less than 1 km) impedance heterogeneities. From his simultaneous analysis of both direct S waves and their coda from local earthquakes, Kopnichev[16] suggested that wave scattering produced by numerous discrete scatterers, such as cracks in the crust of seismically active regions, plays an important role in coda wave generation. His suggestion is supported by the recent discovery[17–19] that the amplitude decay rate of coda waves changes markedly before and after a large earthquake. Stress variations before and after a large earthquake cause changes in the properties of fractures in the crust, resulting in observable differences in coda decay. Therefore, I believe that the small-scale heterogeneities responsible for the generation of short-period coda waves may be the numerous cracks present in the earth's crust. Accordingly, in the laboratory test for coda generation, I employed small circular holes as crack-like scatterers in the models of scattering media.

In view of the above, I first tested the multiple-scattering model of Gao *et al.* for coda generation in laboratory experiments, then, using their multiple-scattering model analyzed short-period seismic coda waves from local small earthquakes that had taken place in the central Kinki district of southwest Japan. From the results obtained by the coda analysis based on the multiple-scattering theory in the central Kinki district and other regions of the world, I deduced the kind of heterogeneities

responsible for short-period coda generation and their size.

2. Laboratory test of scattering models for seismic coda generation

2.1 Scattering models for coda generation

Several important properties of coda waves are as follows: (1) coda waves are not regular plane waves coming from an epicenter from a small-aperture array observation[20-22]; (2) the power spectra of coda waves from different local earthquakes decay as a function of the lapse time measured from the source origin time independent of the distance and the nature of the path between the epicenter and station[1,2]; (3) this time dependence of the power spectra also is independent of the earthquake's magnitude, at least for small earthquakes of $M<6$[1,2]; (4) the coda shows a stable site effect that is very close to the average site effect of shear waves arriving from various directions, and the site effect measurements of coda waves always display less scatter than do shear waves[4]; (5) for a given local earthquake at an epicentral distance of less than about 100 km the total duration of a seismogram t_{f-p} (the time from the beginning of the P waves to the end of the coda) is independent of the epicentral distance or azimuth and can be used effectively as a measure of earthquake magnitude[23-25].

From these properties of coda waves, Aki[8] concluded that the coda waves from local earthquakes consist of S-to-S back-scattered waves from numerous heterogeneities distributed in the lithosphere. His conclusion is based on the assumptions that the medium is not strongly heterogeneous and that the mean free paths, l, of the waves between the scatterers are greater than the distances traveled, βt, of coda waves from the source to the receiver; i.e., $l>\beta t$, when β is the S-wave velocity and t is the lapse time measured from the source origin time. Assuming that the receiver occupies the same place as the source of primary waves in a three-dimensional infinite elastic medium with random but uniform distribution of isotropic scatterers, the coda power spectral density, $P_{sin}(\omega, t)$, for the single-scattering case can be expressed in the form[2]

$$P_{sin}(\omega, t) = 2\beta^{-1} S(\omega)\, t^{-2} \exp(-\omega t Q^{-1})\, g_{sin} \tag{1}$$

in which $S(\omega)$ is the source factor, ω is the angular frequency and Q is the apparent quality factor. Apparent attenuation, $2\pi Q^{-1}$, represents the fractional loss of energy due to scattering and intrinsic absorption per cycle. By representing the quality factor for scattering by Q_{scat} and that for intrinsic absorption by Q_{ab}, Q can be expressed in terms of Q_{scat} and Q_{ab} in the form[26]

$$Q^{-1} = Q_{scat}{}^{-1} + Q_{ab}{}^{-1}. \tag{2}$$

When η is the apparent (total) attenuation coefficient, g is the scattering coefficient and γ is the absorption coefficient, $\eta=g+\gamma$. Moreover, Q_{scat} and Q_{ab} can be expressed as

$$Q_{scat} = \omega/g\beta \tag{3}$$

and

$$Q_{ab} = \omega/r\beta\,. \tag{4}$$

Eq. (1) shows that the apparent attenuation Q^{-1} is determined uniquely by fitting the decay curve predicted by the single-scattering formula (eq. (1)) to the observed decay curve and further that when $S(\omega)$ is estimated from the spectral analysis of S waves, the scattering coefficient, g_{sin}, as an excitation factor also is determined uniquely by the same method.

The mean free path of the waves between scatterers may not be as great as assumed in single-scattering calculations because the actual medium may be markedly heterogeneous. Therefore, multiple scattering must be taken into account. Kopnichev[13] and Gao *et al.*[14] both formulated the time decay of coda energy density at a hypocenter respectively considering the effect of scattering up to the 3rd and 7th orders. They assumed (a) that primary and scattered waves are of the same type, having a common propagation velocity; i.e., they neglected wave conversions from P to S or S to P; (b) that the isotropic scatterers are distributed randomly and uniformly in an elastic medium; i.e., the scattering is isotropic; (c) that the durations of primary waves are much shorter than the intervals over which coda power is to be estimated; and (d) that scattered waves are incoherent and their energies additive.

When Kopnichev's formula for the coda power spectral density is represented by $P_K(\omega, t)$ and that of Gao *et al.* by $P_G(\omega, t)$, $P_K(\omega, t)$ and $P_G(\omega, t)$ can be expressed[13,14] as

$$P_K(\omega, t) = 2\beta^{-1} S(\omega) t^{-2} \exp(-\omega t Q^{-1})\, g_K(1+0.61\varepsilon+0.15\varepsilon^2) \tag{5}$$

and

$$P_G(\omega, t) = 2\beta^{-1} S(\omega) t^{-2} \exp(-\omega t Q^{-1})\, g_G(1+1.23\varepsilon e^{0.33\varepsilon}), \quad \varepsilon = g\beta t, \tag{6}$$

in which g_K and g_G are the isotropic scattering coefficients for each formula and ε is the ratio of the distance traveled, βt, of coda waves from the source to the receiver to the mean free path, $l(=1/g)$, of the waves between the scatterers. Eqs. (5) and (6) show that in multiple-scattering the apparent quality factor (Q) and the scattering coefficient (g) are not determined uniquely as they are in single-scattering.

As described above, ε is the ratio of the distance traveled, βt, of coda waves to the mean free path l; thus, scattering is weak for $\varepsilon<1$, whereas it is strong for $\varepsilon>1$. Therefore, we can use the value of ε as a measure of the strength of scattering. Coda power ratios, P_{sin}/P_G (dashed curve) and P_K/P_G (solid curve) are shown in **Fig. 1** as a function of ε, on the assumption that $g_{sin}=g_K=g_G$. This figure shows that when ε is about 0.65, the coda power excited by single scattering is equal to that excited by scattering from the 2nd to 7th order; i.e., $P_{sin}/P_G=0.5$.

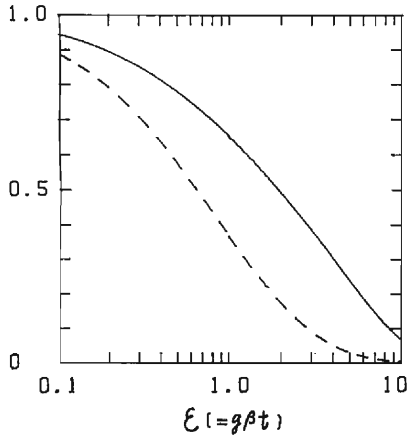

Fig. 1. Coda power ratios as a function of ε: solid curve, P_K/P_G; dashed curve, P_{sin}/P_G; ε, ratio of the distance traveled to the mean free path g^{-1}. P_{sin}, P_K and P_G denote coda power spectral densities by Aki and Chouet[2], Kopnichev[13] and Gao *et al*[14].

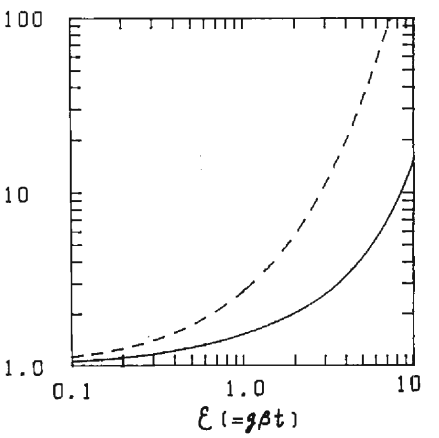

Fig. 2. Ratios of scattering coefficients (g) as a function of ε: solid curve, g_K/g_G; dashed curve, g_{sin}/g_G; ε, ratio of the distance traveled to the mean free path g^{-1}.

This means that, when $\varepsilon>0.65$, the contribution of scattering greater than the 2nd order to the coda dominates the power spectral density. But, single scattering well accounts for coda power when $\varepsilon<0.65$. I here define the critical value of ε as 0.65, at which $P_{sin}/P_G=0.5$, as ε_c. In contrast, when ε is about 2, $P_K/P_G=0.5$. Thus, for $\varepsilon>2$ the contribution of scattering greater than the 4th order to the coda dominates the power spectral density.

Comparisons of the factors for coda excitation produced by scattering in eqs. (1), (5) and (6) show the following relations;

$$g_{sin} = g_G(1+1.23\varepsilon e^{0.33\varepsilon}) \tag{7}$$

and

$$g_K = g_G(1+1.23\varepsilon e^{0.33\varepsilon})/(1+0.61\varepsilon+0.15\varepsilon^2)\,. \tag{8}$$

Ratios of the scattering coefficients, g_{sin}/g_G (dashed curve) and g_K/g_G (solid curve) are shown in **Fig. 2** as a function of ε. The discrepancy between g_{sin} and g_G depends on the value of ε. For $\varepsilon<\varepsilon_c$, g_{sin} agrees roughly with g_G, whereas for $\varepsilon>\varepsilon_c$ the discrepancy is marked. In contrast, g_K agrees roughly with g_G for $\varepsilon<2$, whereas for $\varepsilon>2$ the discrepancy between g_K and g_G is marked.

Thus, the coda power ratio, P_{sin}/P_G, and the ratio of the scattering coefficients, g_{sin}/g_G, as a function of ε show that, for $\varepsilon<\varepsilon_c$ the single-scattering model for coda generation is valid, but for $\varepsilon>\varepsilon_c$ the multiple-scattering model must be used to analyze coda amplitude. Similarly, Kopnichev's model is valid for $\varepsilon<2$, but is not ap-

plicable for $\varepsilon > 2$.

The theory of Gao *et al.* also predicts a coda decay rate that is more gradual than that from the single-scattering model for large lapse times; i.e., for $t \gg t_c$. They concluded that multiple scattering would cause estimates of the coda Q derived from the single-scattering model to be 1.5 times that of the transmission Q of the medium if the loss in power produced by intrinsic absorption in the medium is considered negligible.

2.2 Laboratory tests of the scattering models

The scattering models for coda wave generation were tested in ultrasonic model experiments that used two-dimensional model media. As stated in section 1, the small-scale heterogeneities considered responsible for short-period coda generation may be numerous discrete scatterers such as cracks in the crust of seismically active regions. Therefore, small circular holes were used as scatterers in the models of scattering media tested.

A block flow diagram of the apparatus used is shown in **Fig. 3.** The transmitter and receiver were made of PZT ceramics and had diameters of 4 mm and the same resonance frequency, f (f=200–250 KHz). When the transmitter is excited by one output pulse from the pluse generator, it emits an ultrasonic wave to the medium of the model; the other output pulse of the pulse generator is used as a shot mark. The ultrasonic wave travels through the medium of the model then is picked up by the receiver. The received signals pass through the pre-amplifier with a gain of 40 dB and through the low-pass filter with a variable cut-off frequency, then they are stored in digital memory with a capacity and resolution of 4 kwords and 8 bits. The wave then can be analyzed by a micro-computer system. The standard error in the measurements of wave amplitude was within 6% when the transmitter was fixed during the experiments and 9% when the transmitter was reset with every measurement. The counter was used to measure the travel time. The start and stop pulses that controlled the counter were the output pulse of the pulse generator. The stop pulse,

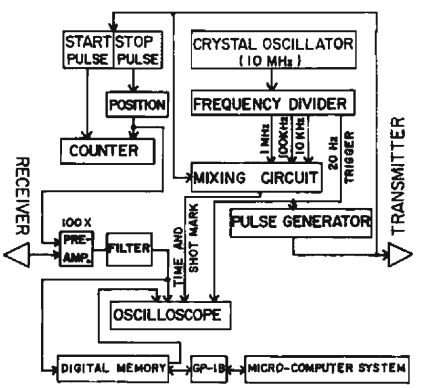

Fig. 3. Block diagram of the experimental apparatus.

shaped like a spike, was set at the onset time of a P wave monitored on an oscilloscope. The resolution of the counter was ± 0.1 microsecond. Wave velocity was determined from the travel time curves, the standard error being within 1%.

A sufficiently large duralumin plate 200 cm long, 100 cm wide and 0.2 cm thick was used to produce seismograms with long codas. A large number of random circular holes with diameters of 1.8 mm were drilled over the entire duralumin plate. The positions of the holes on the plate (the ordinates and abscissas) were determined from a list of random numbers. The average number of circular holes per a unit area (1 cm^2) of plate was one, therefore the average distance between each circular hole was about 1 cm. In this way, a model of a scattering medium that had a large number of small circular holes as scatterers was made and denoted Model-A.

The S-wave absorption coefficient, γ, for the duralumin plate has been reported elsewhere[27]. The γ and Q_{ab} values calculated from eq. (4) for $f=200$ KHz and 250 KHz are listed in **Table 1.** The velocity, β, and the scattering coefficient, g, of the S waves were measured in Model-A for $f=200$ KHz and 250 KHz. The scattering coefficient was determined as follows: First, the total apparent attenuation caused by scattering and the intrinsic absorption from amplitude diminution with distance were measured by the diagonal sounding method as in a previous study[28]. Next, the attenuation produced by the absorption of the duralumin plate was subtracted from the total apparent attenuation. The g values obtained had standard deviations of about 30%. The measured g and β values and the Q_{scat} values calculated from eq. (3) for $f=200$ KHz and 250 KHz are listed in **Table 1.** As shown in this table, when 200-KHz S waves travel through Model-A, the model can be considered a scattering medium with $Q=300$ ($Q_{scat}=520$). For 250-KHz S waves, Model-A can be considered a scattering medium with $Q=150$ ($Q_{scat}=220$).

A schematic diagram of the experiment is shown in **Fig. 4.** The transmitter

Table 1. Medium parameters of models used in laboratory experiments

Model	Frequency	S-Wave Velocity	Scattering Coefficient	Absorption Coefficient	Quality Factor Caused by Scattering	Quality Factor Caused by Absorption	Apparent Quality Factor
	f KHz	β Km/sec	g cm^{-1}	γ cm^{-1}	Q_{scat}	Q_{ab}	Q
A	200	3.0	0.008	0.006	520	700	300
A	250	3.0	0.024	0.010	220	520	150

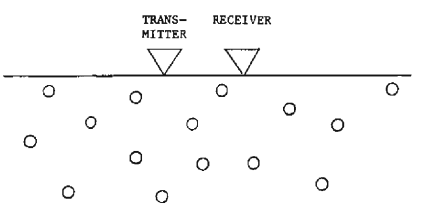

Fig. 4. Schematic diagram for measurements.

and receiver are set on one of the longer edges (sides) of the model. The distance between the transmitter and receiver is about 4 cm. Because the transmitter acts as an impulsive force normal to the edge of the model, it radiates both P and S waves to the medium of the model; Rayleigh waves also are generated and travel along the edge of the model. The energy radiated as S waves is several times that radiated as P waves. Moreover, according to the scattering theory[29], when the scatterer size is smaller than the wave length, both P and S waves generate intensively scattered S waves. In my experiments, the ratio of the hole diameter to the wave length is 0.13 for f=200 KHz and 0.17 for 250 KHz. Thus, the coda waves in my experi-

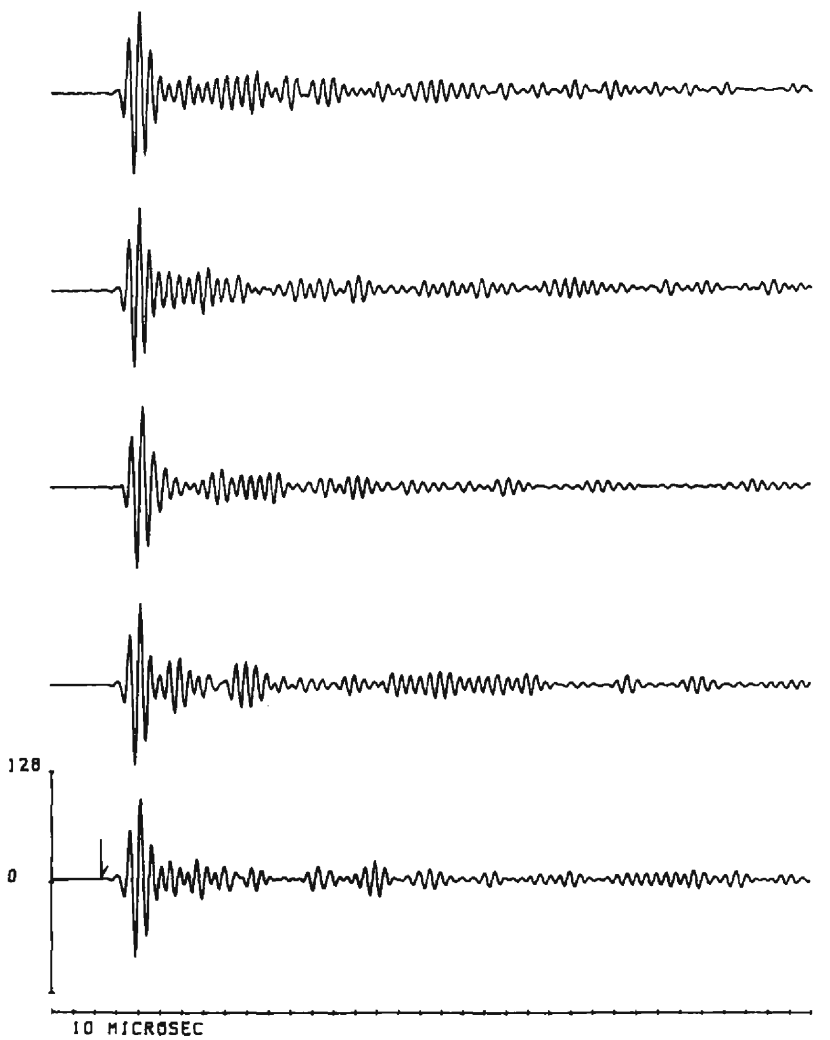

Fig. 5. Seismograms produced by model experiments for medium of Q=300 (g=0.008 cm^{-1} and Q_{scat}=520): the source origin time is marked with a vertical arrow.

ments mostly consisted of S waves scattered singly or multiply by the numerous small circular holes. I observed these coda waves at ten different points along the edge of the model, moving the transmitter and receiver simultaneously.

Examples of seismograms produced in the model medium with $Q=300$ ($g=0.008\ \mathrm{cm}^{-1}$ and $Q_{scat}=520$) are given in **Fig. 5.** Similarly, **Figure 6** shows seismo-

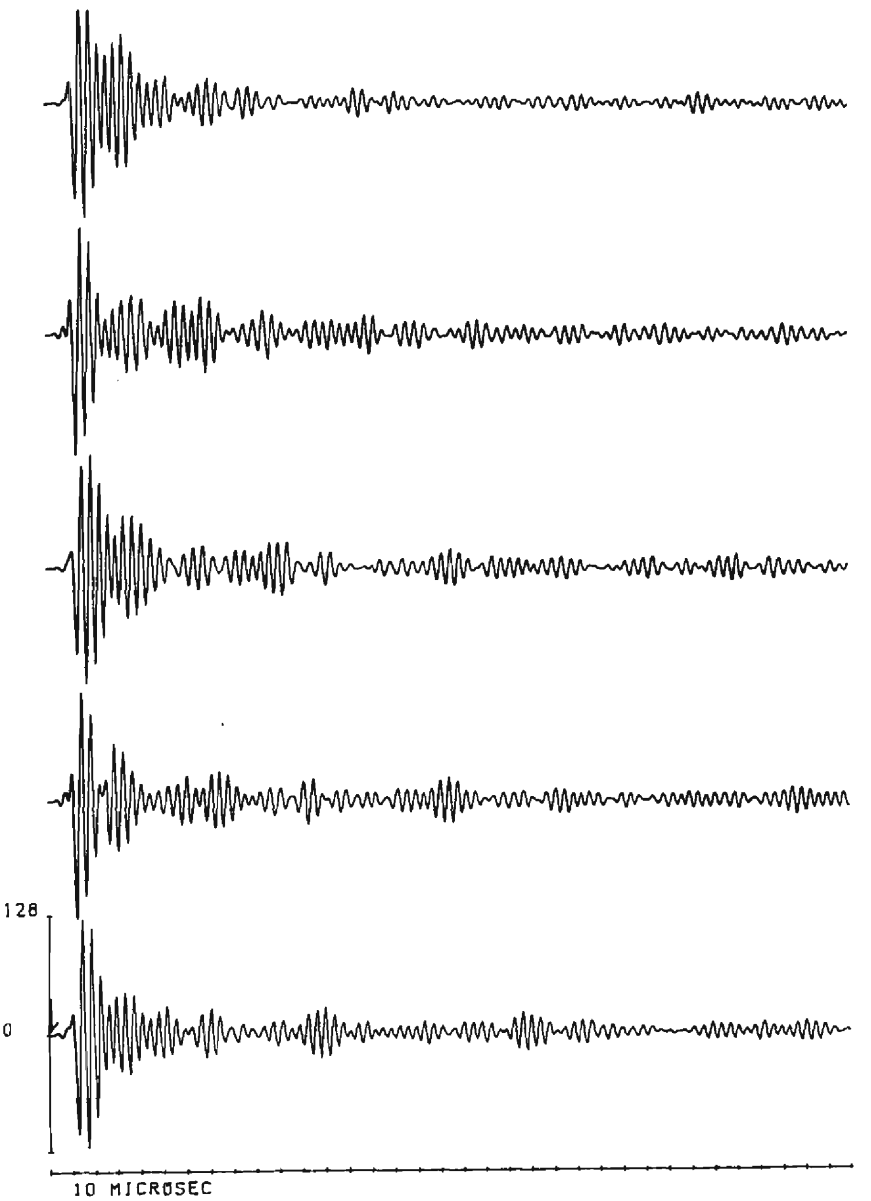

Fig. 6. Seismograms produced by model experiments for medium of $Q=150$ ($g=0.024\ \mathrm{cm}^{-1}$ and $Q_{scat}=220$): the source origin time is marked with a vertical arrow.

grams for the model medium with $Q=150$ ($g=0.024$ cm^{-1} and $Q_{scat}=220$). In these figures, the source origin time is marked by a vertical arrow. Wavelets with large amplitudes in the early parts of the seismograms are direct Rayleigh wavelets. The seismograms are not contaminated by these Rayleigh wavelets at $t>60$ microsec nor by reflected waves from the edges of the model at $t<350$ microsec; therefore, the coda waves could be analyzed for the lapse time of $60<t<350$ microsec.

As seen from eqs. (1) and (6), the amplitude decay rate of the coda depends on the apparent quality factor, Q, and the scattering coefficient, g; whereas, the amplitude of the coda depends on the source factor, $S(\omega)$, the scattering coefficient, g, and the coupling between the transducers and the model medium. Only the amplitude decay rate of the coda was analyzed. The coda amplitude first was normalized to the peak amplitude of the Rayleigh wavelets to remove any effect produced by the source factor and the coupling between the transducers and the model medium on the coda amplitude. Next, the rms (root mean square) amplitude, $A_{r.m.s.}$, of the coda waves was calculated using a moving window whose width was five times the period of the coda waves, and the natural logarithm, $lnA_{r.m.s.}$, of the rms amplitude was obtained. **Figures 7-(a)** and **(b)** show the time decay curves of $lnA_{r.m.s.}$ which are averages of the decay curves observed at ten different points, for model media with $Q=300$ and $Q=150$.

When the geometrical spread of the wave front is two-dimensional, the formula for the single-scattering model for coda generation and that of Gao *et al.* for the multiple-scattering model are[30] respectively

$$P_{sin}(\omega, t) = S(\omega)t^{-1} \exp(-\omega t Q^{-1})\, g_{sin} \tag{9}$$

and

$$P_G(\omega, t) = S(\omega)t^{-1} \exp(-\omega t Q^{-1})\, g_G(1+\varepsilon e^{0.26g}) . \tag{10}$$

When coda decay curves predicted by the single- and multiple-scattering theories are obtained by substituting the Q and g values of the model medium into these formulas (eqs. (9) and (10)), the scattering models for coda generation can be examined from comparisons of coda decay curves observed experimentally and those predicted theoretically. The dashed curve in **Fig. 7-(a)** shows the amplitude decay predicted by the single-scattering theory, while the solid curve shows that predicted by the multiple-scattering theory of Gao *et al.* Comparisons of the observed and theoretically predicted decay curves of coda amplitude show that for a medium with $Q=300$ ($g=0.008$ cm^{-1}) both the single- and multiple-scattering models explain the observed coda decay for $70<t<320$ microsec well.

Figure 7-(b) shows similar results for a model medium with $Q=150$ ($g=0.024$ cm^{-1}). The scattering for this medium is stronger than for the medium with $Q=300$ ($g=0.008$ cm^{-1}). The decay curve (dashed curve) predicted by the single-scattering model begins to disagree with the observed decay curve from about $t=150$ microsec, whereas that (solid curve) predicted by the model of Gao *et al.* agrees well

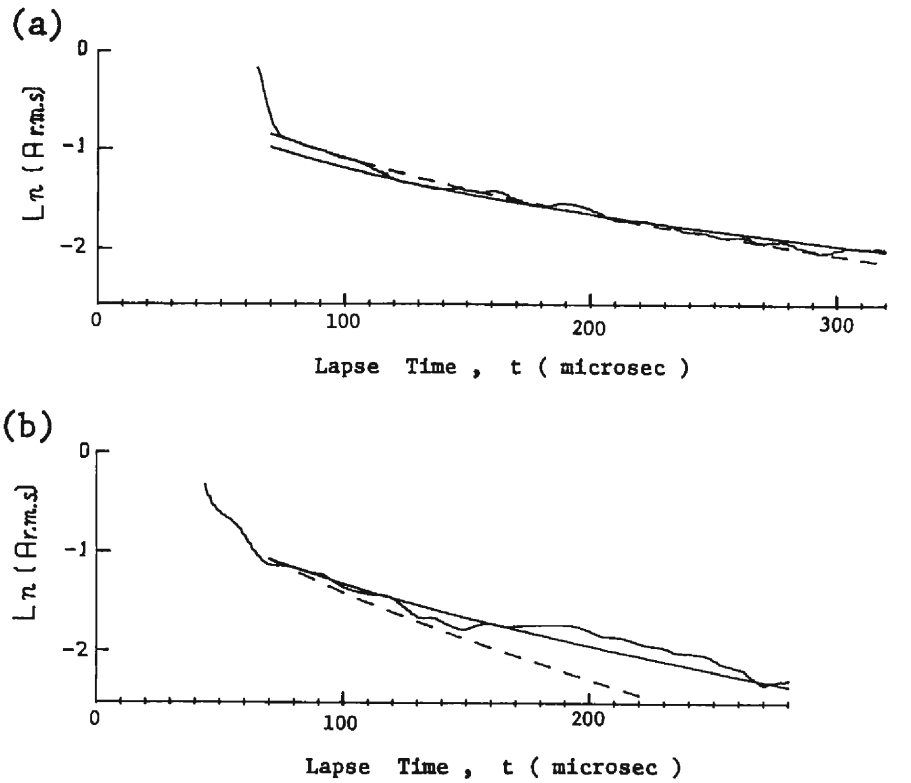

Fig. 7. Observed and predicted coda decays with time. (a) for medium with $Q=300$ ($g=0.008$ cm^{-1} and $Q_{scat}=520$); (b) for medium with $Q=150$ ($g=0.024$ cm^{-1} and $Q_{scat}=220$). Solid curves denote coda amplitude decays predicted by the multiple-scattering model of Gao *et al.* and dashed curves by the single-scattering model.

with the observed decay curve over the entire lapse time analyzed.

As shown in section 2.1 the $\varepsilon(=g\beta t)$ values can be used as a measure of the strength of scattering. In two-dimensional problems, the critical value, ε_c, at which the coda power excited by single scattering is equal to that excited by scattering from the 2nd to 7th order, is 0.8[30]. The critical lapse time, t_c, at which the coda decay curve predicted by the single-scattering model begins to disagree with the observed curve, can be obtained, when the ε_c value and the relation $\varepsilon_c=g\beta t_c$ are used. The predicted t_c then can be compared with the observed value. As shown in **Fig. 7-(a)**, for a model medium with $Q=300$ ($g=0.008$ cm^{-1}), the single-scattering model can be used for the entire lapse time analyzed, $70<t<320$ microsec. The predicted t_c value of about 330 microsec shows that the single-scattering model is applicable at $t<330$ microsec. As seen from **Fig. 7-(b)**, for a model medium with $Q=150$ ($g=0.024$ cm^{-1}), the single-scattering model is not applicable at $t>140$ microsec. The predicted t_c value in this instance is about 110 microsec, which agrees well with the observed value. Thus, the experimental results show that the critical lapse time, t_c, can be used to determine the lapse time range in which the single-scattering

model is applicable.

Model experiments for elastic wave motion generally requires that $D=VT$, in which D, V and T are the scale factors of dimension, velocity and time between the actual medium (or actual seismograms) and the model medium (or model seismograms), respectively. The S-wave velocity (=3 km/sec) of Model-A is nearly the same as the crustal S-wave velocity, i.e., $V=1$. Accordingly, D is nearly equal to $T(D\cong T)$. When both D and T are 10^5, 1 cm in the model is equivalent to 1 km on the earth, and 10 microsec and 100 KHz in the model seismograms are equivalent to 1 sec and 1 Hz on the seismograms. Similarly, when both D and T are 10^4, 1 cm in the model is equivalent to 0.1 km on the earth, and 10 microsec and 100 KHz in the model seismograms are equivalent to 0.1 sec and 10 Hz on the seismograms. Accordingly, the analyzed range of the lapse time, $t<350$ microsec, corresponds to ranges of $t<35$ sec and $t<3.5$ sec on the seismograms for $D=T=10^5$ and $D=T=10^4$, respectively. To analyze the coda in longer lapse time ranges, the scale factors, 10^5, of both dimension and time were used here. The coda parts of the seismograms in the lapse time range of $t<35$ sec are considered to consist of scattering waves from crustal heterogeneities.

From the ratio of S-wave amplitude spectra to the source factor of the coda and from the amplitude ratio of the different frequency bands, Akamatsu[31] showed that the quality factor, Q_β, for S waves is approximated by $Q_\beta=110f^{0.5}$ for the S-wave travel times of $t_s=5$–50 sec in the frequency range of $1<f<20$ Hz for the earth's crust in the Kinki district of southwest Japan. When Dainty's model[26] of a scattering medium in which $Q^{-1}={Q_{ab}}^{-1}+g\beta/\omega$, and in which g is taken as a constant and Q^{-1} is considered to converge at a frequency-independent ${Q_{ab}}^{-1}$ value in the high-frequency limit, is used, and Q is assumed to be approximated by Q_β, a rough estimate of the scattering coefficient, g, can be made from eqs. (2) and (3) and the Q_β values. Furthermore, the critical lapse time, t_c, for the underlying crust of the Kinki district, can be estimated from the g values and the relation $\varepsilon_c=g\beta t_c$. When the Q_{ab} value is assumed to be approximated by a Lg-Q value, 2000[32], in the eastern U.S., a tectonically inactive region and β is 3.3 km/sec, $g=0.024$ km^{-1} and $t_c=8$ sec at 2 Hz. At higher frequencies, the critical lapse time becomes less than that at 2 Hz. This indicates that it is not proper to use the single-scattering model in the lapse time range of $t>8$ sec at frequencies higher than 2 Hz in the analysis of coda waves from local small earthquakes in the Kinki district.

As stated in section 2.1, the theory of Gao *et al.*[14] predicts that at longer lapse times $t\gg t_c$, determination of the quality factor Q from the single-scattering theory overestimates the Q values by a factor of 1.5 (by a factor of 1.4 for two-dimensional problems), if the loss in power owing to intrinsic absorption in the medium is considered negligible. For a model medium with $Q=150$ ($g=0.024$ cm^{-1}), the coda decay curve predicted by the single-scattering model does not agree with the observed curve at $t>140$ microsec (**Fig. 7-(b)**). When the Q value is estimated from the best fit of the decay curve predicted by the single-scattering model to the observed curve,

a Q value of about 260 is obtained, which is larger than the Q value of the model medium by a factor of about 1.7. Experimentally this means that neglect of multiple scattering produces an overestimation of the value of Q.

Because the multiple-scattering model of Gao *et al.* explains the results of experiments well, in which the models of scattering media used had small-scale crack-like scatterers and had g values of 0.008 and 0.024 km^{-1} (cm^{-1}), close to the crustal scattering coefficient, their model can be used to investigate the properties of scattering by numerous cracks in the earth's crust and the apparent attenuation Q^{-1} of the earth's crust using seismic coda waves.

3. Analysis of seismic coda by the multiple scattering model

Local small earthquakes that occurred in the central Kinki district of southwest Japan were analyzed. These were observed by the telemetry network system for microearthquake observation at the Regional Center for Earthquake Prediction of the Faculty of Science, Kyoto University. The magnitudes, M_{JMA}, were between 2.7 and 3.8 (JMA: Japan Meteorological Agency), the focal depths less than 12 km and the epicentral distances from 3 to 23 km. The earthquakes analyzed are listed in **Table 2**, along with the calculated epicentral distances and azimuths from the source locations determined by the Regional Center for Earthquake Prediction. **Figure 8** shows the epicenters of the earthquakes analyzed and the stations in the seismic network.

A vertical component of the seismograms from a three-component velocity seis-

Table 2. List of earthquakes analyzed

Earth-quake No.	Earthquake Code No.	Date	Time h : m	Depth Km	Magnitude M_{JMA}	Station	Epicentral Distance Km	Azimuth N°E
1	EQ01YGI	Mar. 16 1980	11:39	4	3.4	YGI	18	−138
1	EQ01TNJ					TNJ	18	120
2	EQ03KGM	Apr. 8 1980	15:53	8	2.8	KGM	12	85
3	EQ04YGI	Apr. 23 1980	4:30	10	2.7	YGI	10	142
4	EQ09KHK	Oct. 26 1980	5:57	12	3.2	KHK	16	42
4	EQ09BHO					BHO	10	− 65
5	EQ10MYO	Feb. 3 1981	18:25	10	3.8	MYO	3	111
5	EQ10YGI					YGI	17	−175
6	EQ11MYO	Feb. 3 1981	23:05	11	2.9	MYO	3	110
7	EQ12KHK	Feb. 19 1981	15:51	11	2.9	KHK	15	−164
7	EQ12YGI					YGI	10	106
8	EQ14YGI	Apr. 18 1981	23:46	11	2.8	YGI	23	151
8	EQ14MYO					MYO	15	105
9	EQ19MYO	Jan. 25 1982	18:15	7	3.0	MYO	7	− 16

M_{JMA}: magnitude on the scale of the Japan Meteorological Agency

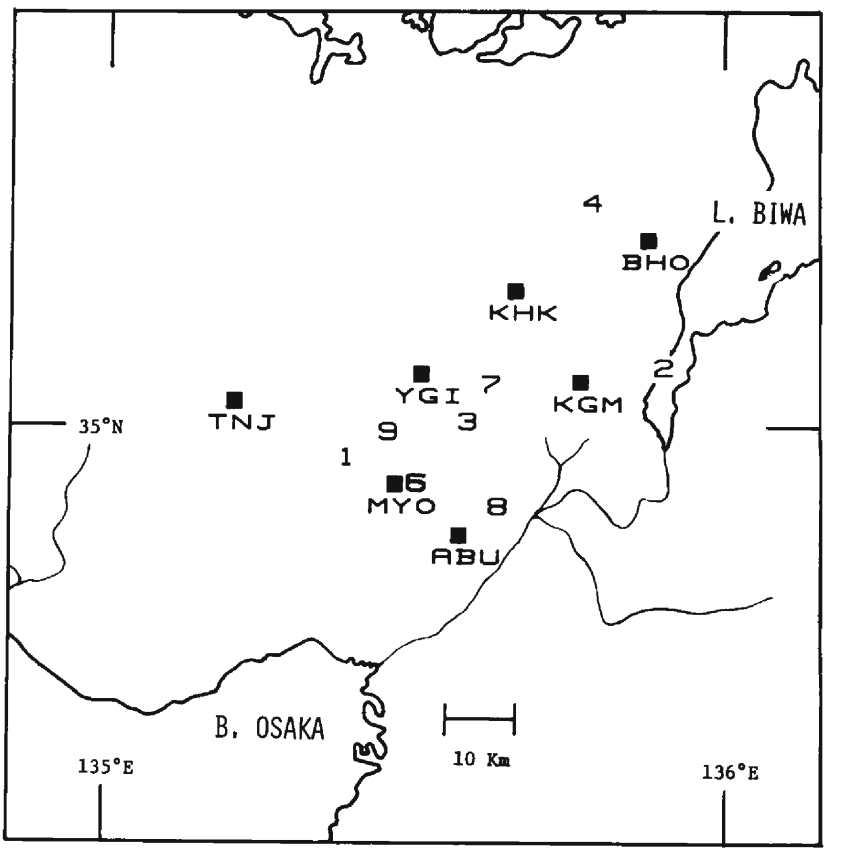

Fig. 8. Epicenters of the earthquakes analyzed and the seismograph stations used for the coda analysis. Epicenters are numbered. The station locations are shown by the solid closed squares.

mometer (1 Hz, 3 volts/kine) was used. Records were digitized at a sampling interval of 5 msec. To examine the dependence of the scattering coefficient on frequency the band-pass-filtered traces were produced by a digital-filtering technique. Their center frequencies were 2, 4, 8 and 16 Hz. Coda waves with frequencies lower than 1 Hz were not analyzed, because surface waves have been reported to have a possible important role in seismic coda at frequencies lower than 1.4 Hz[33]. **Figure 9** shows an example of band-pass-filtered traces.

The rms amplitude $A(f, t)$ was calculated from the filtered records by using a moving window with a width 10 times the wave period. As shown experimentally in section 2, the time decay of coda power is approximated well by the multiple isotropic scattering formula (eq. (6)) of Gao *et al.* Accordingly, the rms amplitude $A(f, t)$ is

$$A(f, t) \propto t^{-1} \exp(-\pi f t Q^{-1})\, g(1+1.23 g\beta t e^{0.33 g\beta t}) . \tag{10}$$

Taking the natural logarithm of both sides in eq. (10), we obtain

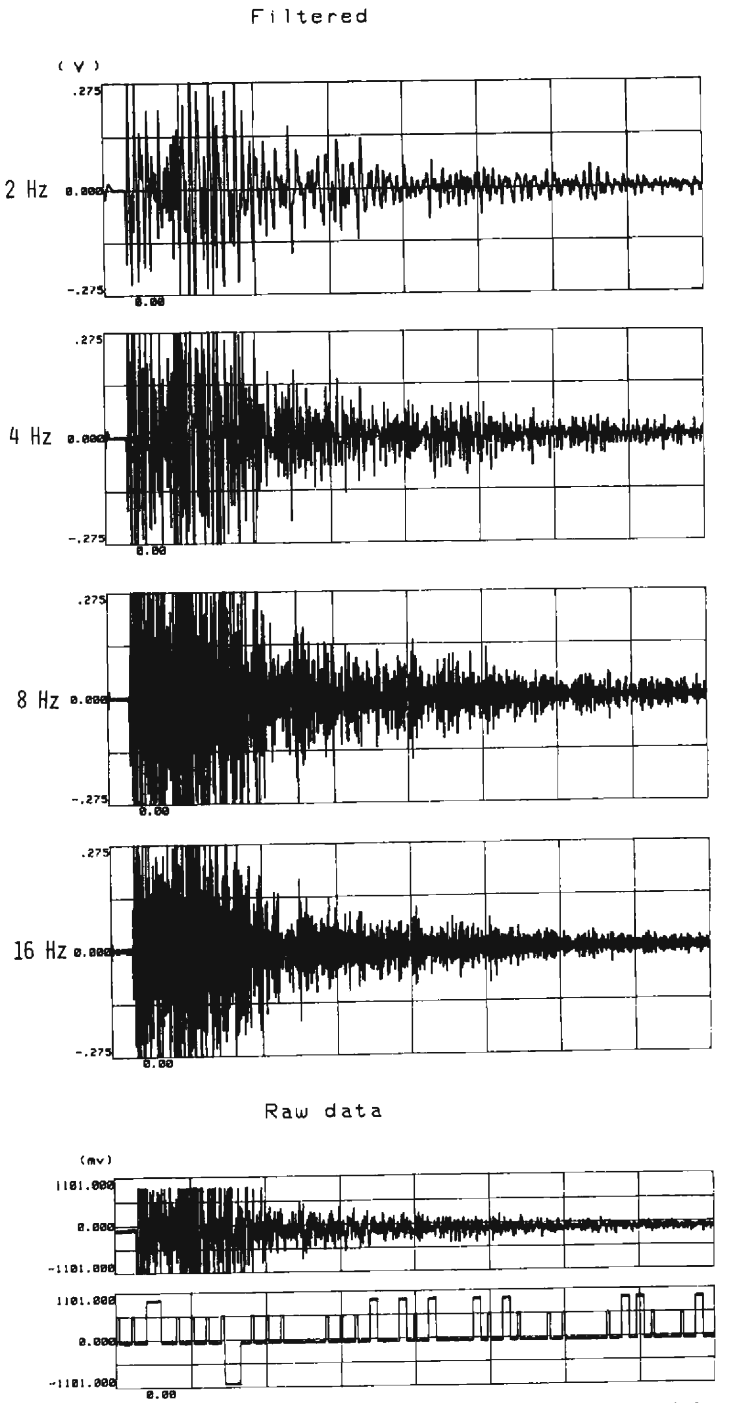

Fig. 9. Band-pass-filtered seismograms. This earthquake (No. 4) was recorded at BHO. The center frequencies of the band-pass filters are indicated on the left of the figure.

$$lnA(f, t) = C - lnt - \pi f Q^{-1} t + lng(1 + 1.23 g\beta t e^{0.33 g\beta t}), \quad (11)$$

in which C is an arbitrary constant.

Assuming that the value of Q is approximated by the apparent quality factor, Q_β, of the S waves[31], the scattering coefficient, g, can be uniquely determined from the best fit of the observed coda decay to eq. (11). The analyzed lapse time is from $2t_s$ to about 35–40 sec, t_s denoting the travel time of the direct S waves. The t_s values of the analyzed earthquakes range from about 3 to 7 sec; therefore, the lower limit of $2t_s$ for the analyzed interval is roughly 10 sec. The upper limit of the analyzed interval is restricted to about 35–40 sec because the model experiments in section 2 showed that coda decay with time is explained well by the multiple isotropic scattering model of Gao *et al.* for the lapse times of $t<35$ sec. The amplitude at $t=40$ sec is more than 10 times that of the noise before and after the earthquake in each filtered record. Thus, the analyzed interval for any event is roughly 30 seconds, from 10 to 40 sec.

Figure 10 shows an example of the natural logarithmic rms amplitude $lnA(f, t)$ and the decay curves fitted to $lnA(f, t)$ with eq. (11) on the assumption that $Q=$

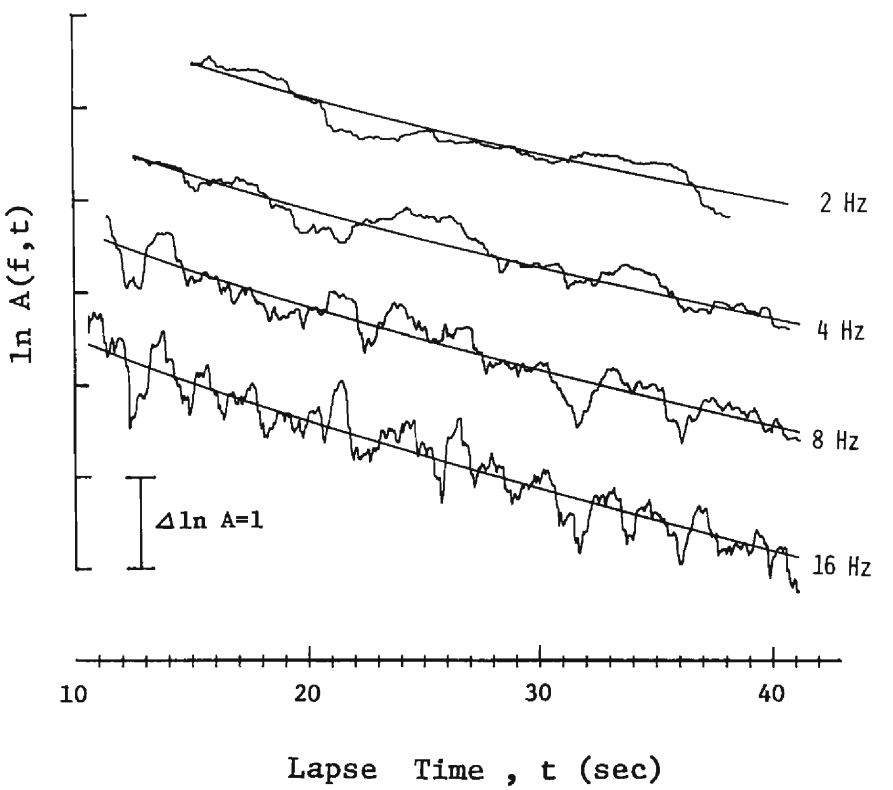

Fig. 10. Natural logarithmic rms amplitudes $lnA(f, t)$ and decay curves best fitted to the $lnA(f, t)$ obtained with the multiple-scattering formula (eq. (11)).

$Q_\beta = 110 f^{0.5}$. The values of the scattering coefficient, g, obtained by fitting eq. (11) to the observed coda decay, are listed in **Table 3.** **Figure 11** gives those g values (denoted by circles) as a function of frequency and shows that g is nearly proportional

Table 3. Estimations of the scattering coefficient g (Km^{-1}) in the central Kinki district

Region	Frequency, f (Hz)			
	2	4	8	16
Kinki District	16.2±7.5	39±15	73±18	143±24

Values are for $g \times 10^3$. Uncertainties (±) are the standard errors.

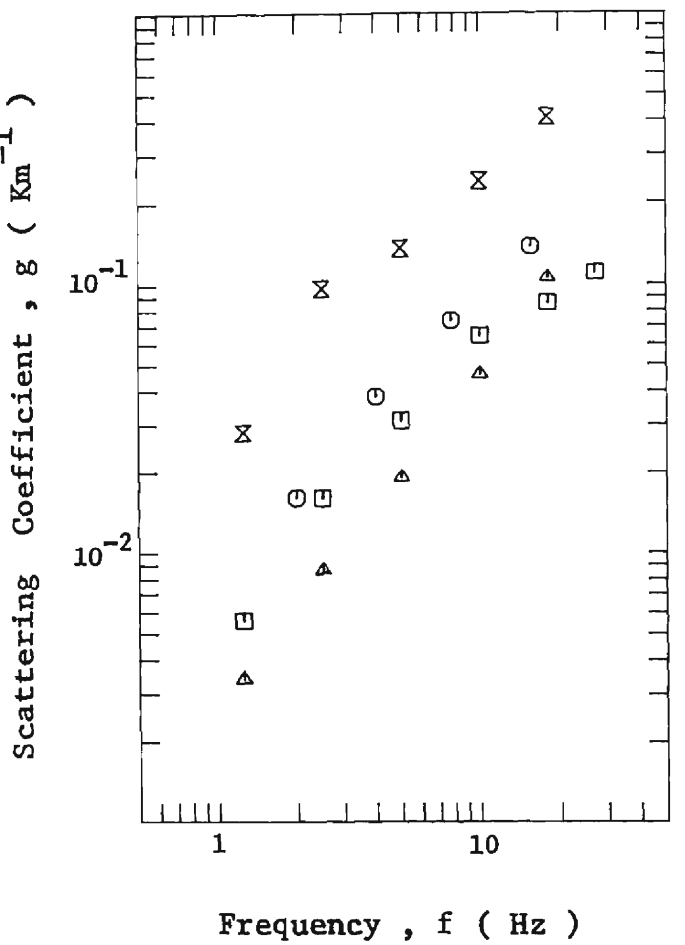

Fig. 11. Dependence of the scattering coefficient, g, on frequency: circles, the central Kinki district; squares, the Northern Garm region; paired triangles, the Southern Garm region; triangles, the Northern T'ienshan region.

to $f^{1.0}$. The kind of heterogeneities responsible for coda generation and their sizes can be deduced from the frequency dependence obtained for the scattering coefficient.

4. Discussion

The model experiments showed that the multiple-scattering model for coda generation reported by Gao *et al.* explains the time decay of coda consisting of scattering waves from small-scale crack-like heterogeneities in the earth's crust very well. The scattering coefficient, g, was nearly proportional to $f^{1.0}$ in the frequency range of $2<f<16$ Hz from the analysis of coda waves from local small earthquakes in the central Kinki district made with the multiple-scattering model for coda generation. Kopnichev[16] also obtained g proportional to $f^{0.7-1.2}$ in the Garm and northern T'ienshan regions of the U.S.S.R. from his simultaneous analysis of direct S waves and their coda for local earthquakes made with his multiple-scattering model for coda generation. The g values for the Garm and northern T'ienshan regions of the U.S.S.R. are listed in **Table 4.** Scattering coefficients (g) are given as a function of frequency for the central Kinki district, and for the Garm and northern T'ienshan regions in **Fig. 11**, which shows that the frequency dependence of g has strong similarities in these regions and that g is roughly proportional to $f^{1.0}$.

So far, two types of lithosphere model as scattering media have been used. One is the "random medium" model, in which the parameters of the medium fluctuate randomly in space around their mean values. This model is characterized by small perturbations of the elastic constants and of the density. Thus, this type of scatterer shows weak contrast to the surrounding averaged field. The second type is the "randomly distributed specific scatterers" model. It assumes scatterers of a specific type (e.g., cracks[34]) which show great contrast to the surrounding medium. In the former model, the scattering coefficient is proportional to $f^n(n=4)$ in the low-frequency range[29,35] ($ka<1$), but in the intermediate- and high-frequency ranges ($ka>1$) it shows a frequency dependence that varies with the correlation function of the random parameters of the medium[15,36], when f is the wave frequency and ka is 2π the ratio of the heterogeneity size, a, to the wave length $2\pi/k$. In the latter model, the frequency dependence of g has yet to be investigated in detail.

Table 4. Estimations of the scattering coefficient g (Km^{-1}) in the Garm and Northern T'ienshan regions of the U.S.S.R. (by Kopnichev[16])

Region	Frequency, f (Hz)					
	1.25	2.5	5.0	10.0	18.0	27.0
Northern Garm	5.3±1.3	16 ± 5	31±10	64±24	85±31	110±37
Southern Garm	28 ±3.0	97 ±16	135±25	240±57	410±94	
Northern T'ienshan	3.4±1.0	8.8±1.3	19± 7	46±21	107±34	

Values are for $g\times 10^3$. Uncertainties (±) are the standard errors.

Although the problem treated theoretically by Kikuchi[34] is for a simple case (for the scattering of S waves in a two-dimensional medium with many infinitesimally thin cracks perpendicular to the direction of wave propagation), his results can be used to roughly estimate crack distribution in fractured media such as seismically active regions. Kikuchi's principal result is that in fractured media the scattering coefficient takes a peak value at $kL=\pi$, when kL is 2π the ratio of the crack length, L, to the wave length, $2\pi/k$. Moreover, according to the model experiment reported by Strizhkov and Ponyatovskaya[37] for elastic wave scattering by randomly distributed cracks, which used an ultrasonic technique and three-dimensional models of cracked media, g is nearly proportional to $f^n(n\simeq 1)$ and has a peak at about $kL=3$–4[38].

These theoretical and experimental results suggest that for scatterers that are in strong contrast to the surrounding medium, the dependence of g on frequency becomes weak; i.e., the value of n in the form of $g\propto f^n$ in the low-frequency range becomes smaller. Therefore, assuming that the lithosphere is a scattering medium with randomly distributed heterogeneities, because of the weak dependence of g on frequency in the earth's crust in seismically active regions, such as the central Kinki district, the Garm and northern T'ienshan regions, it is suggested that the heterogeneities responsible for short-period coda generation may be numerous small-scale cracks present in the earth's crust. On the assumption that the g values in the central Kinki district have peaks at frequencies higher than 16 Hz and that the S-wave velocity is 3.3 Km/sec, a rough estimate of the mean length of these cracks, based on the results of Kikuchi[34] and of Strizhkov and Ponyatovskaya[37], shows that the mean crack lengths in that district are smaller than 100 m.

I have assumed that the apparent attenuation coefficient, η, defined as $\eta=g+r$, is approximated by the apparent attenuation coefficient, $\alpha(=\omega/\beta Q_\beta)$, for S waves. When we compare the scattering coefficient, g, with the apparent attenuation coefficient, $\alpha(=\omega/\beta Q_\beta)$, of the S waves, α is larger than, or comparable to, g at 2–4 Hz; but, at 8–16 Hz it is considerably smaller. This unreasonable property at 8–16 Hz is explained by the theoretical evidence[39] that α is usually smaller than η and depends on the relative magnitudes of the scattering and absorption coefficients. This was first shown by Wu[39] who derived a formulation of seismic energy transfer under multiple scattering by using the radiative transfer theory and who discussed the possibilities of using this approach to separate scattering and intrinsic attenuation. According to his formulation, the energy density $E(r)$ of the direct waves observed is composed of two terms. The first term is the coherent energy density $E_c(r)$ that decays exponentially with distance, the extinction coefficient as its attenuation coefficient being $\eta(=g+r)$. The second term is the diffuse energy density, $E_d(r)$, generated by scattering, in which r is the travel distance. In isotropic scattering, the $E(r)-r$ curves (the energy density distribution along the travel path) have very different shapes depending on the values of $B_0(=g/(g+r))$. For strong scattering ($B_0>0.5$), the apparent attenuation coefficient α, measured from the slope

of the $E(r)-r$ curve, is much smaller than the extinction coefficient η; $\alpha<\eta$. This is because $E_d(r)$ is dominant in $E(r)$. For weak scattering ($B_0<0.5$), the effect of scattering on the apparent attenuation is less appreciable; $\alpha\cong\eta$. Accordingly, scattering attenuation appears to be dominant in seismic wave attenuation at frequencies higher than 4 Hz, at least in my study.

Seismic coda waves of local earthquakes generally are believed to be irregular (incoherent) waves coming from various directions. Recently, from his polarization analysis of the coda waves of small earthquakes in the Garm and northern T'ienshan regions of the U.S.S.R., Kopnichev[40] concluded that coda waves are composed of linearly polarized regular waves and irregular waves with no polarization. He also reported that the regular waves dominant during large lapse times ($t>200$ sec) are S waves reflected from horizontal velocity discontinuities in the upper mantle and that the irregular waves dominant at a small t are single- or multiple-scattered waves from crustal heterogeneities. Furthermore, it has been also reported[33] that coda wavelets with large wave-energy have elliptical polarizations. The polarization of the coda waves of small earthquakes requires a more careful study in relation to the model for seismic coda generation.

I analyzed coda waves for the lapse time of $10<t<40$ sec, the period when coda waves mostly travel in the earth's crust, and deduced that these coda mostly consist of irregular scattered waves.

5. Conclusions

In summary, the principal results obtained are

1. The ultrasonic model experiments done demonstrate that the multiple-scattering model of Gao *et al.* for coda generation explains very well the time decay of coda that consist of waves scattered by small-scale crack-like heterogeneities present in the earth's crust.
2. When the lithosphere is assumed to be a scattering medium with randomly distributed heterogeneities, the isotropic scattering coefficient, g, of the earth's crust in the central Kinki district is nearly proportional to $f^{1.0}$ in the frequency range of $2<f<16$ Hz.
3. From the weak dependence of g on frequency, such as $g\propto f^{0.7-1.2}$, for the earth's crust in seismically active regions, it is suggested that the heterogeneities responsible for short-period coda generation may be the numerous cracks present in the crust with lengths smaller than 100 m.

Acknowledgments

I thank Prof. Soji Yoshikawa and Associate Prof. Kojiro Irikura of Kyoto University for their critical readings of my manuscript and for their valuable suggestions on carrying out my research. I am also indebted to Miss Keiko Amano for complet-

ing my manuscript.

References

1) Aki, K.: Analysis of the Seismic Coda of Local Earthquakes as Scattered Waves, J. Geophys. Res., Vol. 74, 1969, pp. 615–631.
2) Aki, K. and B. Chouet: Origin of Coda Waves; Source, Attenuation and Scattering Effects, J. Geophys. Res., Vol. 80, 1975, pp. 3322–3342.
3) Sato, H.: Energy Propagation Including Scattering Effects; Single Isotropic Scattering Approximation, J. Phys. Earth, Vol. 25, 1977, pp. 27–41.
4) Tsujiura, M.: Spectral Analysis of Coda Waves from Local Earthquakes, Bull. Earthquake Res. Inst., Tokyo Univ., Vol. 53, 1978, pp. 1–48.
5) Roecker, S. W., J. King and D. Hatzfeld: Estimation of Q in Central Asia as a Function of Frequency and Depth Using Locally Recorded Earthquakes, Bull. Seism. Soc. Am., Vol. 72, 1982, pp. 129–149.
6) Rautian, T. G. and V. I. Khalturin: The Use of Coda for Determination of the Earthquake Source Spectrum, Bull. Seism. Am., Vol. 68, 1978, pp. 923–948.
7) Biswas, N. N. and K. Aki: Characteristics of Coda Waves: Central and Southcentral Alaska, Bull. Seis. Soc. Am., Vol. 74, 1984, pp. 493–507.
8) Aki, K.: Attenuation and Scattering of Short-Period Seismic Waves in the Lithosphere, In Identification of Seismic Sources; Earthquake or Explosion, E. S. Husebye and S. Mykkeltveit, Editors, D. Reidel, Hingham, Massachusetts, 1981, pp. 515–541.
9) Akamatsu, J. and K. Matsunami: Effects of Multiple Scattering on Seismic Coda Waves, Abstr. Seism. Soc. Jpn., No. 1, 1985, A66 (in Japanese).
10) Del. Pezzo, E. and A. Zollo: Attenuation of Coda Waves and Turbidity Coefficient in Central Italy, Bull. Seism. Soc. Am., Vol. 74, 1984, pp. 2655–2659.
11) Frankel, A. and R. W. Clayton: Finite Difference Simulations of Seismic Scattering: Implications for the Propagation of Short-Period Seismic Waves in the Crust and Models of Crustal Heterogeneity, J. Geophys. Res., Vol. 91, 1986, pp. 6465–6489.
12) Menke, W. and R. Chen: Numerical Studies of the Coda Fall-off Rate of Multiply Scattered Waves in Randomly Layered Media, Bull. Seism. Soc. Am., Vol. 74, 1984, pp. 1605–1621.
13) Kopnichev, Yu. F.: The Role of Multiple Scattering in the Formation of a Seismogram's Tail, Izv., Earth Physics, No. 8, 1977, pp. 72–77 (in Russian).
14) Gao, L. S., N. N. Biswas, L. C. Lee and K. Aki: Effects of Multiple Scattering on Coda Waves in Three-Dimensional Medium, Pure and Apll. Geophys., Vol. 121, 1983, pp. 3–15.
15) Wu, R. S. and K. Aki: Elastic Wave Scattering by a Random Medium and the Small-Scale Inhomogeneities in the Lithosphere, J. Geophys. Res., Vol. 90, 1985, pp. 10261–10273.
16) Kopnichev, Yu. F.: Determination of Attenuation and Scattering by a Combined Analysis of Regular Waves and Coda, Izv., Earth Physics, No. 1, 1982, pp. 48–62 (in Russian).
17) Gusev, A. A. and V. K. Lemzikov: The Anomalies of Small Earthquake Coda-Wave Characteristics before the Three Large Earthquakes of the Kurile-Kamchatka Zone, Volcanology and Seismology, No. 4, 1984, pp. 76–90 (in Russian).
18) Jin, A., T. Cao and K. Aki: Regional Change of Coda Q in the Oceanic Lithosphere, J. Geophys. Res., Vol. 90, 1985, pp. 8651–8659.
19) Sato, H.: A Precursorlike Change in Coda Excitation before the Western Nagano Earthquake (M_s=6.8) or 1984 in Central Japan, J. Geophys. Res., Vol. 92, 1987, pp. 1356–1360.
20) Aki, K., M. Tsujiura, M. Hori and K. Goto: Spectral Study of Near Earthquake Waves (1), Bull. Earthquake Res. Inst., Tokyo Univ., Vol. 36, 1958, pp. 71–98.
21) Aki, K. and M. Tsujiura: Correlation Study of Near Earthquake Waves, Bull. Earthquake Res. Inst., Tokyo Univ., Vol. 37, 1959, pp. 207–232.
22) Scheimer, J. and T. E. Landers: Short-Period Coda of a Local Event at LASA, Seismic Discrimination, Semiannu. Tech. Sum. 42, Lincoln Lab., MIT, Cambridge, 1974, pp. 17–29.
23) Bisztricsany, E. A.: A New Method for the Determination of the Magnitude of Earthquakes,

Geofiz. Kozlem., Vol. 7, 1958, pp. 69–96.
24) Soloviev, S. L.: Seismicity of Sakhalin, Bull. Earthquake Res. Inst., Tokyo Univ., Vol. 43, 1965, pp. 95–102.
25) Tsumura, K.: Determination of Earthquake Magnitude from the Total Duration of Oscillation, Bull. Earthquake Res. Inst., Tokyo Univ., Vol. 45, 1967, pp. 7–18.
26) Dainty, A. M.: A Scattering Model to Explain Seismic Q Observations in the Lithosphere between 1 and 30 Hz, Geophys. Res. Ltrs. Vol. 8, 1981, pp. 1126–1128.
27) Matsunami, K.: Scattering of P Waves in a Two-Dimensional Model of a Medium with Random Velocity Fluctuations, Annuals, Disas. Prev. Res. Inst., Kyoto Univ., No. 22B–1, 1979, pp. 91–105 (in Japanese).
28) Matsunami, K.: Scattering of P Waves by Random Heterogeneities with Sizes Comparable to the Wave Length, Bull. Disas. Prev. Res. Inst., Kyoto Univ., Vol. 33, 1983, pp. 129–145.
29) Knopoff, L. and J. A. Hudson: Scattering of Elastic Waves by Small Inhomogeneities, J. Acoust. Soc. Am., Vol. 36, No. 2, 1964, pp. 338–343.
30) Gao, L. S., L. C. Lee, N. N. Biswas and K. Aki: Comparison of Single and Multiple Scattering Effects on Coda Waves, Bull. Seism. Soc. Am., Vol. 73, 1983, pp. 377–389.
31) Akamatsu, J.: Attenuation Property of Seismic Waves and Source Characteristics of Small Earthquakes, Bull. Disas. Prev. Res. Inst., Kyoto Univ., Vol. 30, 1980, pp. 53–80.
32) Nuttli, O. W.: Seismic Waves Attenuation and Magnitude Relations for Eastern North America, J. Geophys. Res., Vol. 78, 1973, pp. 876–885.
33) Akamatsu, J. and K. Matsunami: Polarization and Attenuation of Seismic Coda Waves, Annuals, Disas. Prev. Res. Inst., Kyoto Univ., No. 29B–1, 1986, pp. 117–124 (in Japanese).
34) Kikuchi, M.: Dispersion and Attenuation of Elastic Waves due to Multiple Scattering from Inclusions, Phys. Earth Planet. Inter., Vol. 25, 1981, pp. 159–162.
35) Chernov, L. A.: Wave Propagation in a Random Medium, McGraw-Hill, New York, 1960.
36) Sato, H.: Attenuation of S Waves in the Lithosphere due to Scattering by Its Random Velocity Structure, J. Geophys. Res., Vol. 87, 1982, pp. 7779–7785.
37) Strizhkov, S. A. and V. I. Ponyatovskaya: Elastic Wave Scattering by Randomly Distributed Cracks in a Three-Dimensional Medium, Izv., Earth Physics, No. 8, 1984, pp. 72–77 (in Russian).
38) Kopnichev, Yu. F.: Short-Period Seismic Wave Fields, Nauka, M., 1985, pp. 5–139 (in Russian).
39) Wu, R. S.: Multiple Scattering and Energy Transfer of Seismic Waves—Separation of Scattering Effects from Intrinsic Attenuation—I. Theoretical Modeling, Geophys. J. R. Astr. Soc., Vol. 82, 1985, pp. 57–80.
40) Kopnichev, Yu. F.: Seismic Coda Waves, Nauka, M., 1978, pp. 46–53 (in Russian).